YALE PEABODY MUSEUM

JOURNAL OF MARINE RESEARCH

The *Journal of Marine Research,* one of the oldest journals in American marine science, published important peer-reviewed original research on a broad array of topics in physical, biological, and chemical oceanography vital to the academic oceanographic community in the long and rich tradition of the Sears Foundation for Marine Research at Yale University.

An archive of all issues from 1937 to 2021 (Volume 1–79) are available through EliScholar, a digital platform for scholarly publishing provided by Yale University Library at https://elischolar.library.yale.edu/.

Requests for permission to clear rights for use of this content should be directed to the authors, their estates, or other representatives. The *Journal of Marine Research* has no contact information beyond the affiliations listed in the published articles. We ask that you provide attribution to the *Journal of Marine Research.*

Yale University provides access to these materials for educational and research purposes only. Copyright or other proprietary rights to content contained in this document may be held by individuals or entities other than, or in addition to, Yale University. You are solely responsible for determining the ownership of the copyright, and for obtaining permission for your intended use. Yale University makes no warranty that your distribution, reproduction, or other use of these materials will not infringe the rights of third parties.

Linear instability of uniform shear zonal currents on the β-plane

by Nathan Paldor[1], Yona Dvorkin[2] and Doron Nof[3]

ABSTRACT

A unified formulation of the instability of a mean zonal flow with uniform shear is proposed, which includes both the coupled density front and the coastal current. The unified formulation shows that the previously found instability of the coupled density front on the f-plane has natural extension to coastal currents, where the instability exists provided that the net transport of the current is sufficiently small. This extension of the coupled front instability to coastal currents implies that the instability originates from the interaction between Inertia-Gravity waves and a vorticity edge wave and not from the interaction of the two edge waves that exist at the two free streamlines due to the Potential Vorticity jump there. The present study also extends these instabilities to the β-plane and shows that β slightly destabilizes the currents by adding instabilities in wavelength ranges that are stable on the f-plane but has little effect on the growthrates in wavelength ranges that are unstable on the f-plane. An application of the β-plane instability theory to the generation of rings in the retroflection region of the Agulhas Current yields a very fast perturbation growth of the scale of 1 day and this fast growth rate is consistent with the observation that at any given time, as many as 10 Agulhas rings can exist in this region.

1. Introduction

The study of linear instabilities that develop as small amplitude, wavelike, perturbations on a mean current is greatly simplified by assuming that the latter is typified by a uniform lateral shear. In cases where the thickness of the layer of fluid under study vanishes along a contour (e.g. when the isopycnal that bounds the layer from below, shoals until it intersects the ocean's surface along a line commonly referred to as a free streamline) the mean shear has to equal the Coriolis frequency for the mean potential vorticity to be finite (i.e. nonsingular). On the f-plane the assumption regarding the uniform shear (that equals f_0) leads, via the geostrophic balance, to a parabolic sea-surface height in the case of a barotropic ocean (and a parabolic interface depth in the equivalent-barotropic set-up). This physical set-up described above was studied in the past in two cases (both are depicted in Fig. 1): the

1. Fredy and Nadine Herrmann Institute of Earth Sciences, The Hebrew University of Jerusalem, Givat Ram, Jerusalem 91904, Israel, *email: nathan.paldor@huji.ac.il*
2. Geologcial Survey of Israel, Jerusalem 95501, Israel.
3. Department of Earth, Ocean and Atmospheric Science, Florida State University, Tallahassee, Florida, 32306, U.S.A.
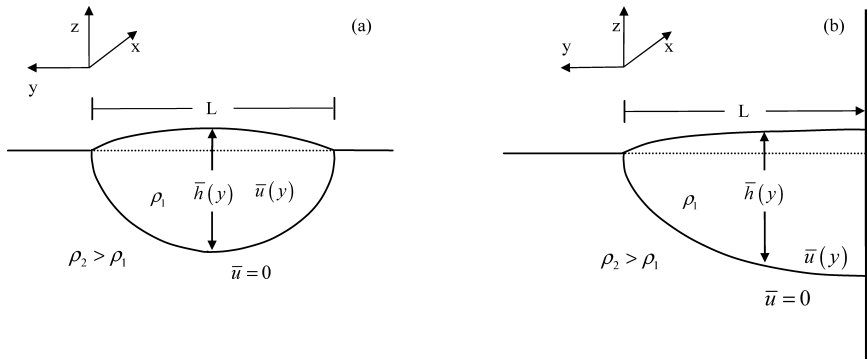
Figure 1. The coupled density front (a, left) and the coastal current (b, right) with uniform mean shear. On the f-plane, geostrophy yields a parabolic interface cross-stream variation. In the coastal current, the flow is uni-directional when the interface slopes monotonically throughout the entire domain whereas a return flow exists near the coast when the slope changes sign, which occurs when the slope of the interface at the free streamline is sufficiently small. The elevation of the sea-surface is greatly exaggerated as it only compensates for the deepening of the interface so as to yield uniform (hydrostatic) pressure in the lower layer. In both cases the mean width of the current is L and a free streamline (where the interface intersects the sea-surface) exists at $y = 0$. In the case of the coastal current (panel b) the coast bounds the current at $y = -L$ while in the case of coupled density front (panel a) a second free streamline exists at $y = -L$.

coupled density front, where the interface that bounds the upper layer intersects the free surface along two lines (panel (a)), and the coastal current where the mean flow is bounded on one side by a vertical wall (panel (b)).

An analytic theory of the instability of a coupled density front was proposed by Griffiths *et al*. (1982, GKS hereafter), where the theoretical estimations (made up of analytical calculations for long waves and their numerical extension to short waves) were compared with laboratory experiments. The original theory of GKS was subsequently extended in Paldor and Ghil (1990) to the two-layer case, where the dynamics of the lower layer is coupled with that of the upper layer by the hydrostatic relation (and this coupling is due to the finite depth of the lower layer). The main new finding of Paldor and Ghil (1990) is the existence of additional instabilities that prevail in discontinuous wavenumber bands. These instabilities exist due to the interaction of other modes rather than those whose interaction generates the instability discovered by GKS. In addition, Paldor and Ghil (1990) have also shown that in a two-layer ocean in which the lower layer is sufficiently thin, a continuous (in zonal wavenumber) instability curve exists for short waves where the growth rate increases linearly with the wavenumber. Recently, Scherer and Zeitlin (2008) have demonstrated numerically that the isolated instability bands of the coupled density front originate from the coalescence of real modes: Inertia-gravity modes; standing modes (where the real part of the phase speed vanishes) and vorticity modes (associated with potential vorticity discontinuity at the free streamlines).

In the case of the uniform shear current, shown in panel (b) of Figure 1, Paldor (1983) showed that this current is stable on the f-plane provided that the flow is uni-directional and its minimal speed is above some threshold value. However, the numerical search has not detected any instability even when the current has a retrograde segment near the coast (i.e. a part of the current that flows backwards relative to the off-coast part) so its mean speed is below the threshold value. This case was extended to a two-layer set-up in Paldor and Ghil (1991), and a continuous unstable mode was found for sufficiently shortwave perturbations. However, the stability of this current was never investigated on the β-plane.

Despite the different boundary conditions, the two uniform shear cases are analyzed in the present study in a single theory. We use a unified formulation that applies to both the coastal current case, where the physical boundary condition is "no normal flow" at the coast and the coupled density front, where the physical boundary condition at the right free streamline is regularity of the solutions. This unified formulation is applied to the instability study of the two cases on the β-plane, where both the mean flows and the perturbation equations are more cumbersome than on the f-plane.

The paper is organized as follows: The unified formulation of the instability problem of the uniform shear flow on the β-plane in the two cases is developed in Section 2. In Section 3 we deduce analytical constraints of the instability theory on the f-plane and in Section 4 we calculate numerically the instabilities that follow from this unified formulation. The study ends with a discussion in Section 5.

2. A unified formulation of the instability problem of coastal currents and coupled density fronts

We consider the Shallow Water Equations (SWE) on the β-plane:

$$\frac{\partial u}{\partial t} + u\frac{\partial u}{\partial x} + v\frac{\partial u}{\partial y} - v(f_0 + \beta y) = -g\frac{\partial h}{\partial x},$$

$$\frac{\partial v}{\partial t} + u\frac{\partial v}{\partial x} + v\frac{\partial v}{\partial y} + u(f_0 + \beta y) = -g\frac{\partial h}{\partial y},$$

$$\frac{\partial h}{\partial t} + \frac{\partial (hu)}{\partial x} + \frac{\partial (hv)}{\partial y} = 0. \tag{1}$$

where, (x, y) are the Cartesian coordinates in the (east, north) directions, t is time, (u, v) are the components of the velocity vector in the (x, y) directions, h is the thickness of the layer, and g is the gravitation constant. The Coriolis frequency, f, is assumed to vary linearly with y i.e., $f = f_0 + \beta y$, with $f_0 = 2\Omega\sin(\phi_0)$ and $\beta = 2\Omega\cos(\phi_0)/R$ (where ϕ_0 is the central latitude of the domain and R and Ω are Earth's radius and frequency of rotation, respectively).

We let L denote the mean width of the current in both the coupled front and the coastal current (see Fig. 1), and use it for scaling the horizontal lengths (x, y). Scaling time on $1/f_0$ leads naturally to the velocity scale $f_0 L$ and selecting $(f_0 L)^2/g$ to be the height scale

completes the scaling that transforms the dimensional system (1) into the nondimensional form:

$$\frac{\partial u}{\partial t} + u\frac{\partial u}{\partial x} + v\frac{\partial u}{\partial y} - v(1 + \varepsilon y) = -\frac{\partial h}{\partial x},$$

$$\frac{\partial v}{\partial t} + u\frac{\partial v}{\partial x} + v\frac{\partial v}{\partial y} + u(1 + \varepsilon y) = -\frac{\partial h}{\partial y},$$

$$\frac{\partial h}{\partial t} + h\frac{\partial v}{\partial y} + v\frac{\partial h}{\partial y} + h\frac{\partial u}{\partial x} + u\frac{\partial h}{\partial x} = 0, \tag{2}$$

where $\varepsilon = \frac{\beta L}{f_0} = \cot(\phi_0)\frac{L}{R}$. For $L \approx 400$ km and $\cot(\phi_0) \approx 1.6$ (near $35°$ latitude) the small parameter ε is about 0.1. At higher latitudes (poleward of $35°$) and for narrower (less than 400 km) currents the value of ε is smaller than 0.1.

We now assume that a basic (mean) state exists, and that it is made up of $\bar{u}(y), \bar{h}(y)$ that are in geostrophic balance with no x or t dependence. Small amplitude (linear) perturbations about this basic state are the focus of the search for instabilities. Since the geostrophic balance of the mean flow, $\bar{u}(y) = -\frac{1}{1+\varepsilon y}\frac{\partial \bar{h}}{\partial y}$, provides only one relationship between $\bar{u}(y)$ and $\frac{\partial \bar{h}(y)}{\partial y}$, another constraint is needed to uniquely determine both $\bar{u}(y)$ and $\bar{h}(y)$. In previous similar instability studies on the f-plane (GKS; Paldor and Ghil, 1990, 1991) the additional constraint was imposed as a uniform shear, i.e. $\partial \bar{u}/\partial y = Const$. The dimensional value of this uniform shear of the mean flow in these studies was chosen to be f_0. Accordingly, in the present (nondimensional) formulation we set $\bar{u}(y)$ to equal $y + U_0$ for some constant U_0 (which is an arbitrary velocity at $y = 0$) so as to ensure that for $\varepsilon = 0$ our results can be compared to those obtained in the previous studies. The mean flow is then:

$$\bar{u}(y) = y + U_0$$

$$\bar{h}(y) = -\frac{\varepsilon y^3}{3} - \frac{y^2}{2}(1 + \varepsilon U_0) - U_0 y = -\frac{y^2}{2} - U_0 y - \varepsilon\left(\frac{y^3}{3} + U_0\frac{y^2}{2}\right)$$

From the last expression for the mean thickness it is clear that $\bar{h}(-1) = U_0 - \frac{1}{2} + \varepsilon(\frac{1}{3} - \frac{U_0}{2})$ so for $\bar{h}(-1)$ to be nonnegative (the thickness of the upper layer can not be negative), U_0 has to satisfy $U_0 \geq \frac{1-\frac{2\varepsilon}{3}}{2-\varepsilon}$. For $U_0 = \frac{1-\frac{2\varepsilon}{3}}{2-\varepsilon} = \frac{3-2\varepsilon}{6-3\varepsilon} \approx \frac{1}{2}(1 - \frac{1}{6}\varepsilon)$ (and in particular $U_0 = 0.5$ for $\varepsilon = 0$) the mean height vanishes at the right boundary, $y = -1$ (in addition to the left boundary, $y = 0$) and the coupled density front is recovered. It is clear from the definition of $\bar{u}(y)$ that it is uni-directional for $U_0 \geq 1$, while for $U_0 < 1$ there is a segment near $y = -1$ where it is negative (directed towards $-x$).

Having determined the basic state we now turn our attention to the perturbations. Since there are no coefficients in the SWE that depend explicitly on x or t (only f depends on y), one can safely let the perturbations take the form of zonally propagating waves with y-dependent amplitudes: $(u, v, h) \sim (u(y), v(y), h(y))e^{ik(x-ct)}$.

Substituting this form in the (linearized) perturbation equations and defining $V = -ikv \Leftrightarrow v = V \frac{i}{k}$ one obtains:

$$uc = u\bar{u} - \frac{\varepsilon y V}{k^2} + h,$$

$$Vc = \bar{u}V - (1 + \varepsilon y)u - \frac{\partial h}{\partial y},$$

$$hc = \frac{\bar{h}}{k^2}\frac{\partial V}{\partial y} - \frac{V}{k^2}\bar{u}(1 + \varepsilon y) + \bar{u}h + \bar{h}u.$$

These equations can be written as a matrix-like eigenvalue system where the phase speed, c, is the eigenvalue and $(u(y), V(y), h(y))$ is the eigenvector:

$$\begin{pmatrix} \bar{u} & -\frac{\varepsilon y}{k^2} & 1 \\ -(1 + \varepsilon y) & \bar{u} & -\frac{\partial}{\partial y} \\ \bar{h} & -\frac{\bar{u}(1+\varepsilon y)}{k^2} + \frac{\bar{h}}{k^2}\frac{\partial}{\partial y} & \bar{u} \end{pmatrix} \begin{pmatrix} u \\ V \\ h \end{pmatrix} = c \begin{pmatrix} u \\ V \\ h \end{pmatrix} \tag{3}$$

(the differential operator, $\partial/\partial y$, that appears in some of the elements of the matrix is the reason why this is not a genuine matrix eigenvalue problem).

Since the first of these equations (the upper row of the matrix) does not contain the differential operator, this algebraic relationship actually expresses u as a linear combination of h and V:

$$u = -\frac{h}{(\bar{u} - c)} + \frac{\varepsilon y V}{k^2(\bar{u} - c)}.$$

This simple expression can be employed to eliminate u from the other two equations, which yields the pair of coupled differential equations:

$$\frac{\partial h}{\partial y} = V\left[\bar{u} - c - \frac{\varepsilon y}{k^2(\bar{u} - c)} - \frac{\varepsilon^2 y^2}{k^2(\bar{u} - c)}\right] + h\left[\frac{1}{(\bar{u} - c)} + \frac{\varepsilon y}{(\bar{u} - c)}\right],$$

$$\frac{\partial V}{\partial y} = V\left[\frac{\bar{u}}{\bar{h}}(1 + \varepsilon y) - \frac{\varepsilon y}{(\bar{u} - c)}\right] + h\left[-\frac{k^2}{\bar{h}}(\bar{u} - c) + \frac{k^2}{(\bar{u} - c)}\right]. \tag{4}$$

The last step in the formulation of the problem is the transformation of this (h, V) system to a new (h, ψ) system where the variable ψ is defined by: $\psi = V \cdot \bar{h}$. The resulting new system is:

$$\frac{\partial h}{\partial y} = \frac{\psi}{\bar{h}}\left[\bar{u} - c - \frac{\varepsilon y}{k^2(\bar{u} - c)} - \frac{\varepsilon^2 y^2}{k^2(\bar{u} - c)}\right] + h\left[\frac{1 + \varepsilon y}{(\bar{u} - c)}\right],$$

$$\frac{\partial \psi}{\partial y} = \psi\left[-\frac{\varepsilon y}{(\bar{u} - c)}\right] + h\left[-k^2(\bar{u} - c) + \frac{\bar{h}k^2}{(\bar{u} - c)}\right]. \tag{5}$$

The main advantage of the transformation from V to ψ is that the boundary conditions associated with system (5) are $\psi(0) = 0 = \psi(-1)$ for both the coupled density front and the coastal current. In contrast, in the (h, V) system the BC at the right boundary is $V(-1) = 0$ in the case of the coastal current and that $V(-1)$ is regular in the case of the coupled density front. The (h, ψ) system lets one analyze the instability of the coupled density front as a particular case of the coastal current's instability where $U_0 = \frac{3-2\varepsilon}{6-3\varepsilon}$ without changing the boundary condition at $y = -1$.

3. Stability of a coastal current on the f-plane

Setting $\varepsilon = 0$ and requiring $U_0 > 0.5$ (i.e. focusing on the coastal current) one can derive integral constraints on the complex solutions of the second order differential eigenvalue system (4) for $c = c_r + i c_i$ with $c_i \neq 0$ (see Eqs. 18 and 19 in Paldor, 1983). These integral constraints lead to the condition:

$$\int_0^1 |\phi|^2 (3z^2 - 2U_0 z - 2|\gamma|^2) dz > 0, \tag{6}$$

where: $z = -y$ (i.e. z varies between 0 and 1), $\gamma = U_0 - c = U_0 - c_r - i c_i$ and $\phi(z(y)) = u(y)$. This integral was used in Paldor (1983) to derive the necessary condition for instability: $U_0 < 3/2$ based on the realization that for $U_0 > 3/2$ the integrand on the left-hand side of (6) is negative throughout the entire $0 \leq z \leq 1$ domain even for vanishingly small γ so the integral inequality cannot be satisfied.

The unified formulation developed in the preceding section provides a natural connection between the instability of the coupled front (where $U_0 = 0.5$) and the coastal current (where $U_0 > 0.5$). By viewing the former problem as a particular case of the latter with $U_0 = 0.5$ it is not clear whether the coastal current is stable throughout the entire $0.5 < U_0 < 1.5$ range (and the instability only occurs for $U_0 = 0.5$) in which case $U_0 > 1.5$ is an overestimate of the stability threshold or there is a whole subrange of $0.5 \leq U_0 < 1.5$ where it is unstable (in which case $U_0 > 1.5$ is a close stability threshold). This f-plane issue is addressed in relation to the total transport of the current, which is also determined by U_0 as follows: For $\bar{h}(-1) = U_0 - 0.5$ and $\bar{h}(0) = 0$ an application of the geostrophic balance to the downstream transport yields:

$$\int_{-1}^0 \bar{h} \cdot \bar{u} \, dy = -\int_{-1}^0 \bar{h} \cdot \bar{h}_y dy = \frac{1}{2}(\bar{h}(-1)^2 - \bar{h}(0)^2) = (U_0 - 0.5)^2/2.$$

For $U_0 = 0.5$ (i.e. the coupled density front) instabilities exist and the total transport vanishes. Whether or not these instabilities prevail for values of U_0 exceeding $1/2$ is unclear from the available literature on the subject and this point is the first point addressed in the next section.

4. Results

The numerical results shown below were calculated using two methods of solutions. The first method applied the Chebyshev collocation method (see a general description of the method in Trefethen (2000) and a particular recent application in De-Leon and Paldor (2011)) to system (3). For the most part, the collocation method was used to solve system (3) with 120 points (a total of 121 points, including the two boundaries) and occasionally verified the accuracy of our results by computing the eigenvalues (i.e. phase speeds) and eigenfunctions (ordered as u, V, and h) with 360 points. The second method is a shooting method where system (5) was integrated numerically from $y = 0$ starting with the initial conditions $\psi(0) = 0$ and $h(0) = 1$ (the latter is a mere trivial normalization value) to $y = -1$ and the value of c was varied in order to find the values for which the boundary condition $\psi(-1) = 0$ is satisfied (see similar application of the shooting method in Paldor and Nof, 1992; Paldor and Dvorkin, 2006). The numerical results obtained with these two methods were identical to more than four significant digits, lying closer to one another than the widths of the curves shown in the figures below but the results of the latter were easier to sort (less spurious roots) and were more robust (to changes of parameters such as accuracy of integration).

The instability curves (growth rates) shown in Figure 2 are an application of the unified instability theory developed in Section 2 to the coupled density front and the coastal current, on the f-plane. Setting $\varepsilon = 0$ in system (5) and letting the value of U_0 increase from 0.5 (the coupled density front; upper panel) to larger values of $U_0 = 0.56$ and $U_0 = 0.62$ (both describe the coastal current, middle and lower panels) we notice that the instability of the coupled density front (the longwave GKS instability, as well as the additional shortwave branches) in which the boundary condition on V is its regularity at $y = -1$, has a natural extension to the coastal current regime despite the change of boundary condition to $V = 0$ at $y = -1$. As the value of U_0 increases from 0.5, the various instability branches shift to the right (shorter waves) and their maximal growth rate decreases. As explained above, U_0 also determines the total transport of the mean current and the results shown in Figure 2 demonstrate that the coastal current is stable from $U_0 \approx 0.65$, at which value its total transport is: $(U_0 - 0.5)^2/2 \approx 0.01$. When U_0 increases above 0.65 the total transport of the coupled current increases above 0.01 and the current becomes stable.

The effect of β (proportional to ε) on the instability of the coupled density front is demonstrated in Figure 3 by calculating the instabilities for $\varepsilon = 0.05$ and $\varepsilon = 0.1$ and setting $U_0(\varepsilon)$ to the appropriate values of the coupled density front: $U_0 = \frac{3-2\varepsilon}{6-3\varepsilon}$. Clearly, on the β-plane, the instability peaks are nearly the sane as those on the f-plane but wavelength ranges that are stable on the f-plane (i.e., the ranges between the isolated peaks in the upper panel of Fig. 2) are destabilized by β.

The β effect is different on the coastal current. As is evident from the results shown in Figure 4, at $U_0 = 0.75$ and $U_0 = 0.65$ (where the coastal current was stable on the f-plane i.e. for $\varepsilon = 0$) the shortwave instability branches near $k = 5.5$ (for $U_0 = 0.65$) and $k = 8.4$ (for $U_0 = 0.75$) become dominant and the separate modes at longer wavelength (see Figs. 2
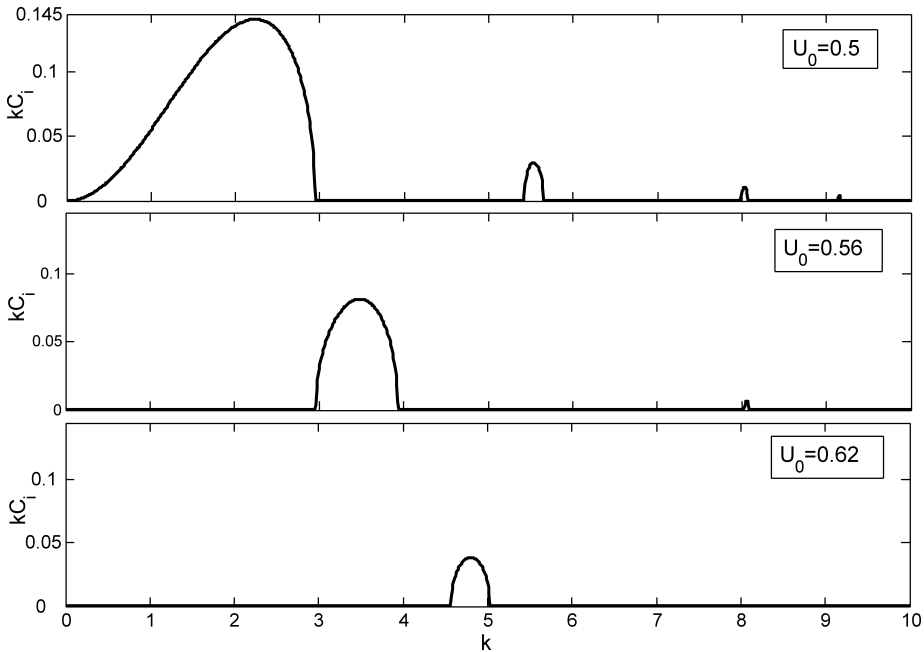
Figure 2. Instability curves, $kC_i(k)$, of the coupled density front ($U_0 = 1/2$, upper panel) and the coastal current ($U_0 > 1/2$, middle and lower panels) on the f-plane ($\varepsilon = 0$). The similarity between the two instabilities is evident despite the different V-boundary condition (but not that of ψ) employed in the two problems. These instabilities vanish for $U_0 \geq 0.65$.

and 3) merge into a single continuous, slightly unstable, mode. The instability curves at $\varepsilon = 0.05$ (not shown) are similar to those at $\varepsilon = 0.1$ but have slightly different central wavenumber and maximal growth rate. No instabilities were found at $U_0 = 0.8$ while at a lower value of $U_0 = 0.6$ this single mode has a somewhat larger amplitude and is located near $k = 0.45$ (which is the central wavenumber of the second peak of the curves shown in Fig. 3). It seems, therefore, that similarly to the variation of the $\varepsilon = 0$ curves in Figure 2 with U_0, in the present $\varepsilon > 0$ case, too, an increase of U_0 from its "coupled front" minimal value eliminates successively the individual peaks of Figure 3.

The (complex) eigenfunctions associated with the unstable modes whose phase speeds were shown above have the expected structure. However, the calculation of the eigenfunction verifies our results regarding the eigenvalues since the former are calculated independently by integrating system (5) numerically using the values of c found previously at the noted values of ε, U_0 and k. An example of the eigenfunction structure is shown in Figure 5 for the instability of the $U_0 = 0.75$ near $k = 8.4$ in Figure 4 and it shows that our numerical solution for $\psi(y)$ satisfies the boundary conditions at $y = -1$ and $y = 0$ and that both $h(y)$ and $\psi(y)$ that solve system (5) are differentiable throughout the $(-1, 0)$ interval.
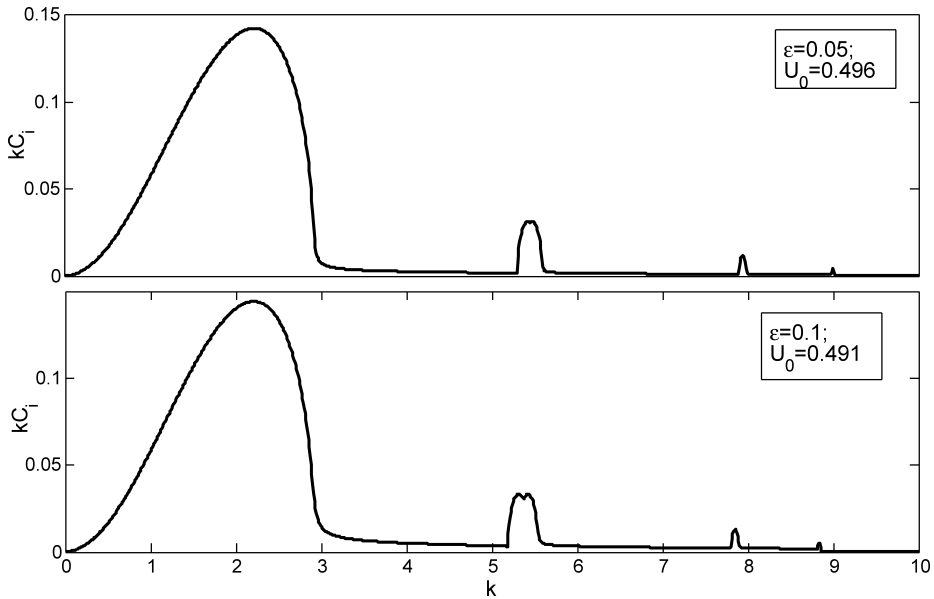
Figure 3. The β-effect (i.e. $\varepsilon \neq 0$) on the instability of the coupled density front (i.e. when $U_0 = (3 - 2\varepsilon)/(6 - 3\varepsilon)$). Clearly, a comparison of these plots with the upper panel of Figure 2 shows that β destabilizes the front in wavelength ranges that are stable on the f-plane but hardly affects the ranges that are unstable on the f-plane.

5. Discussion

The unified formulation proposed here applies to the instability problems of the coupled density front and the coastal current on the f-plane when the shear in both mean flows is uniform. This unified formulation enables one to view the former as a particular case of the latter, and our numerical solutions of Eq. (5) demonstrate that instabilities exist on the coastal current when U_0 is slightly above 0.5 (i.e. $1/2 \leq U_0 \leq 0.65$). Eq. (7) shows that the total downstream transport equals $(U_0 - 0.5)^2/2$ so the disappearance of the instability for $U_0 > 0.65$ occurs when the downstream transport increases above 0.01 at $U_0 = 0.65$.

The results of this study apply to zonal currents only while the f-plane theory of GKS has no similar restriction on the direction of the mean current. The reason for this difference is that on the f-plane all coefficients of the original equations (e.g. system 2 with $\varepsilon = 0$) are constant so that the only nonconstant coefficients in the perturbation equations (system 3 and 4) are those associated with the mean state variables $\bar{u}$ and $\bar{h}$. Accordingly, on the f-plane the directions of x and y remain arbitrary and can be set to fit any observed mean current. In contrast, on the β-plane the explicit dependence of f on y implies that for a mean meridional geostrophic current both $\bar{v}$ and $\bar{h}$ have to be functions of both x and y so the simple scenario portrayed in Section 2 (where $\bar{u}$ and $\bar{h}$ are functions of y only) does not hold.
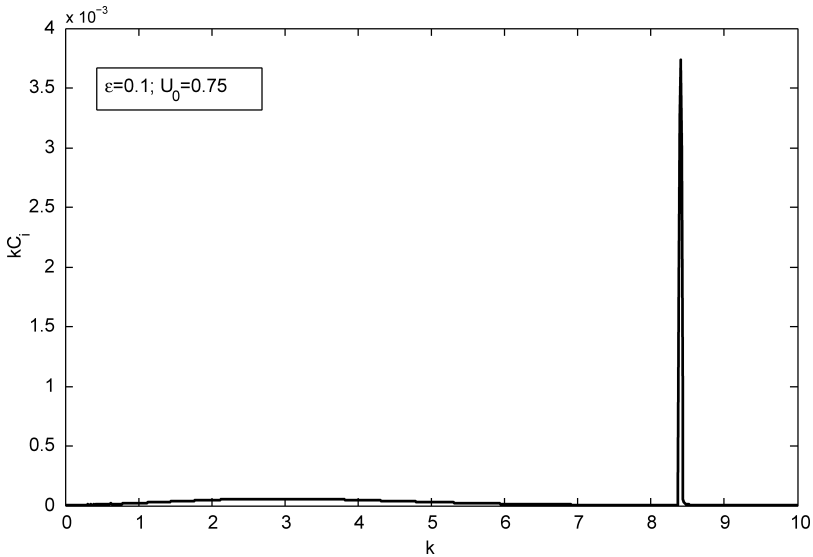
Figure 4. The effect of β (i.e. ε) on the instability of the coastal current at $\varepsilon = 0.1$ and $U_0 = 0.65$; $U_0 = 0.75$, (i.e. above the threshold value of 0.65 above which no instabilities exist on the f-plane). A large range of wavelength becomes slightly unstable and at the narrow range near $k = 5.5$ (for $U_0 = 0.65$) and $k = 8.4$ (for $U_0 = 0.75$) a dominant but narrow branch arises where the maximal growth rates are about 0.025 and 0.0035, which is much larger than the growth rates at lower values of k. The narrow branches with sharp peaks near $k = 5.5$ and $k = 8.4$ are reminiscent of the shortwave branches near $k = 5 - 6$ and $k = 8 - 9$ in Figure 3.

The effect that the variation in f (i.e., the β effect) has on the instability curves is quite different in the two problems: For the coupled density front, β destabilizes the wavenumber ranges that separate the isolated peaks, while hardly affecting the peaks themselves (compare the top panel in Fig. 2 with the two panels of Fig. 3). For the coastal current a single mode exists at $k = 8.4$ for $U_0 = 0.75$ when $\varepsilon = 0.1$ and a wide range instability with small growth rate exists between $k = 0$ and $k = 7$. In contrast, no instability was found in Figure 2 for $U_0 > 0.65$ when $\varepsilon = 0$. This destabilization of short waves is similar to the effect of the lower layer on the coastal current found in Paldor and Ghil (1991).

As was shown in previous studies (e.g. Scherer and Zeitlin, 2008; Paldor and Ghil, 1991) the various instability branches originate from the coalescence of different pairs of real modes in certain wavelength bands, including the particular case when the real part of the phase speed vanishes (e.g. GKS instability) which is interpreted as a standing mode. In the context of the coupled density front, two waves are candidates for this coalescence: Inertia-Gravity (Poincare) waves and vorticity edge (Rossby) waves associated with the PV jump at $y = -1$ and $y = 0$. Our unified formulation and the extension of these instabilities into the $U_0 > 0.5$ region (where only one free streamline exists), imply that in the case of the
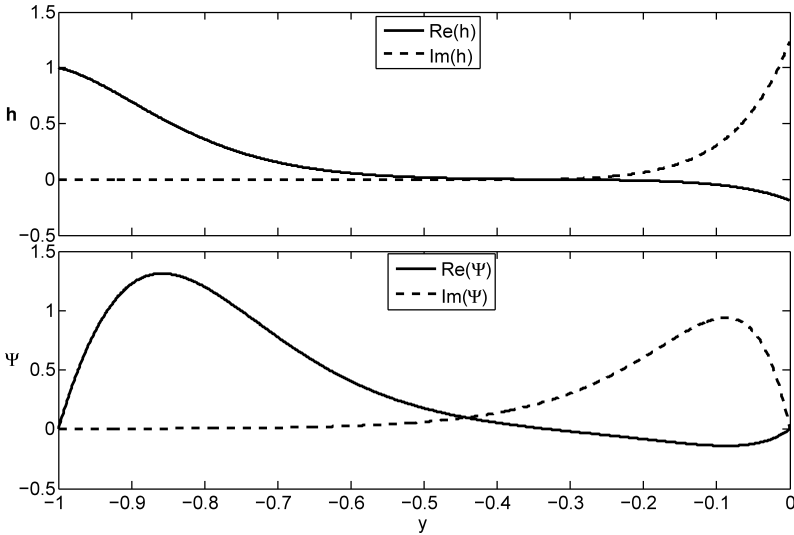
Figure 5. The $(h(y), \psi(y))$ eigenfunctions for $\varepsilon = 0.1$ and $U_0 = 0.75$ at $k = 8.4$ (the "spike" in Fig. 4). The complex phase speed is: $c = 0.414 + 0.44 \cdot 10^{-3}i$ and despite the singularity at $y = -0.336$ of the (real part of the) coefficients $(\bar{u}(y) - c)^{-1} = (U_0 + y - c)^{-1}$ that appear in system (5), the complex eigenfunctions are smooth everywhere, including at the singular point $y = -0.336$.

coupled front ($U_0 = 0.5$) the instabilities result from the interaction Inertia-Gravity waves with an edge wave and not by the interaction of the two edge waves (one at $y = -1$ and the other at $y = 0$). As in other equivalent barotropic instability studies (see e.g. Killworth *et al.*, 1984; Paldor and Killworth, 1987) the energy source for the perturbations' growth is the horizontal shear of the mean current (extracted via the Reinolds stress terms).

The instability theory developed above can be applied to the Agulhas Current near its retroflection point at $35°S - 40°S$ latitude (see Fig. 6.5 in Lutjeharms, 2006). As is evident from the sigma-t 25.8 surface, at this segment the current has zero net transport and two free streamlines, mimicked by the idealized cartoon shown in panel (a) of Figure 1 – the coupled density front. For the relevant oceanographic parameters: L = 300 km (current's mean width at the retroflection region); $\phi_0 =$ south latitude of $37.5°$ one obtains $\varepsilon = \cot(\phi_0)L/R = 0.06$ (so U_0 is about 0.492) and the two lower panels of Figure 3 show that at this ε the current is unstable at all wavelengths. The maximum growth rate in both $\varepsilon = 0.05$ and $\varepsilon = 0.1$ panels occurs at $k = 2.2$ so half the wavelength of the most unstable wave is $(\pi/2.2) * 300$ km ≈ 450 km and the growth rate at $k = 2.2$ (for both values of ε) is 0.15 so the time scale for the growth of the most unstable mode is: $1/(0.15 * f_0) \sim 1$ day. The 450 km estimate of the size of the Agulhas eddies based on half the wavelength of the most unstable mode is consistent with observations of the diameter of rings shed off from the current at the retroflection region (see the discussion on page 170 in Lutjeharms, 2006).

The very fast perturbation growth (about 1 day) is consistent with the observation that more than 10 rings may exist at any given time in the Cape basin just southwest of Cape Town (see Fig.e 6.19 and the discussion on page 173 of Lutjeharms, 2006).

A personal note from Nathan Paldor: I was Melvin Stern's Ph.D. student in the Graduate School of Oceanography of the University of Rhode Island between 1979 and 1982. Melvin proposed the f-plane version of the present study as the topic of my Ph.D. thesis and I am happy to extend Melvin's 30-year-old idea to the β-plane in this tribute to my great mentor and an inspiring scientist. I will always cherish the great moments I had when we discussed various Geophysical Fluid Dynamical problems in the course of my Ph.D. studies and in subsequent years when he moved to FSU and I was a frequent visitor there.

REFERENCES

De-Leon,Y. and N. Paldor. 2011. Zonally propagating wave solutions of Laplace Tidal Equations in a baroclinic ocean of an aqua-planet. Tellus, *63A*, 348–353.

Griffiths, R. W., P. D. Killworth and M. E. Stern. 1982. Ageostrophic instability of ocean currents. J. Fluid Mech., *117*, 343–377.

Killworth, P. D., N. Paldor and M. E. Stern. 1984. Wave propagation and growth on a two-layer geostrophic current. J. Mar. Res., *42*, 761–785.

Lutjeharms, J. R. E. 2006. The Agulhas Current, Springer, 329 pp.

Paldor, N. 1983. Stability and stable modes of coastal fronts. Geophys. Astro. Fluid Dyn., *27*, 217–228.

Paldor, N. and Y. Dvorkin. 2006. Barotropic instability of a zonal jet: From nondivergent perturbations on the β-plane to divergent perturbation on a sphere. J. Phys. Oceanogr., *36*, 2271–2281.

Paldor, N. and M. Ghil. 1990. Finite wavelength instabilities of a coupled density front. J. Phys. Oceanogr., *20*, 114–123.

—— 1991. Shortwave instabilities of coastal currents. Geophys. Astro. Fluid Dyn., *58*, 225–242.

Paldor, N. and P. D. Killworth. 1987. Instabilities of a two-layer coupled front. Deep-Sea Res., *34*, 1525–1539.

Paldor, N. and D. Nof. 1990. Linear instability of an anticyclonic vortex in a two-layer ocean. J. Geophys. Res., *95*(C10), 18,075–18,079.

Scherer, E. and V. Zeitlin. 2008. The instability of coupled geostrophic density fronts and its nonlinear evolution. J. Fluid Mech., *613*, 309–327.

Trefethen, L. N. 2000. Spectral Methods in MATLAB. SIAM, Philadelphia, PA, 165 pp.